



**Powerful Advanced N-Level Digital Architecture**  
for models of electrified vehicles and their components

## Research Innovation Action

GA # 824256

**EUROPEAN COMMISSION**  
**Horizon 2020 | GV-02-2018**

Virtual product development and production of  
all types of electrified vehicles and components

Deliverable No.	PANDA D4.4	
Deliverable Title	Report on the virtual testing of the FCV	
Deliverable Date	2020-12-30	
Deliverable Type	REPORT	
Dissemination level	Public (PU)	
Written By	Fei Gao (UBFC) Eduard-Edis Raclaru (SISW)	2020-12-27 2021-02-19
Checked by	Walter Lhomme (ULille) Gabriel-Mihai Sirbu (RTR)	2021-03-04 2021-02-25
Approved by	Cristir Irimia (WP4 leader) Alain Bouscayrol (coordinator)	2021-04-12
Status	Final version	2020-04-15

## Publishable Executive Summary

Air pollutant emissions from transport are one of Europe's main concerns in controlling the air quality. Emission regulations are in place as part of the EU framework for light-duty and heavy-duty road vehicles. As part of the Horizon 2020 initiative of the European Commission, project PANDA addresses new technological developments to accelerate vehicle electrification which helps protect the environment and reduce the air pollution. The current report belongs to Work Package (WP) 4 of the PANDA project related to electrified vehicle virtual testing. As the result of task 4.4 of WP 4, the current report addresses the system level simulation of fuel-cell electric vehicles.

Technical advancements in fuel-cell based electric vehicles offer an alternative to road vehicles for reducing air pollution. New research and development on fuel-cell vehicles relies on system level simulations to test new vehicle technologies, architectures, and control. Also, system level simulations represent an integrated step in the virtual development of fuel-cell vehicles that helps optimize system design and reduces the costs and time through identifying design flaws early in the development process. In task 4.4, a framework that allows for running fuel-cell vehicle simulations is provided through prebuilt and reconfigurable models of fuel-cell vehicles.

In the PANDA project, the model organization is based on the EMR (Energetic Macroscopic Representation) methodology. Using this representation, models for fuel-cell electric vehicles are developed at the component level and integrated into system level complete vehicle simulations. The purpose of this report is to present the validation of fuel-cell vehicle (FCV) models and to prove the performance of the methodology proposed by using reconfigurable multi-level models.

One of the advantages of the proposed methodology is the flexibility of the simulations, in which components or subsystems models can be replaced with other components or subsystems models, of possibly different complexity, in a seamless manner such that the transition from one type of simulation to another is made easily. In this way, by quickly replacing a subsystem model and adjusting some model parameters, we can perform, through simulation, both subsystem performance tests and global performance tests. In this report, besides the validation of the global vehicle performances, we test the flexibility of the simulation architecture when models are changed.

To prove the accuracy of the models developed, simulation results of the global traction system for the FCV are compared with measured data from a real vehicle. Mobypost is the vehicle that was chosen to perform the tests which were carried on the daily postal delivery track from La Poste by UBFC. Simulations are done using Matlab-Simulink® software and Simcenter Amesim® software provided by the partner SISW. A complete vehicle model of the Mobypost is provided by UBFC by modelling each of the vehicle components using the EMR formalism and integrating them into the complete system model. Validation of the complete vehicle model was done by UBFC, SISW and ULille. The flexibility of the FCV simulations using EMR is tested by replacing the current battery model with other multi-level battery models built by VUB. Thus, the accuracy and efficiency of different simulations was proven, and the model organisation capability was demonstrated.

The comparison between simulated and measured results was done to evaluate the models regarding simulation results precision and time of computation, to ensure a necessary level of quality both for virtual but also real testing.

### Contributions:

No	Who	Description	Date
1	F. Gao (UBFC)	Report creation and outline	2020-12-27
2	F. Gao (UBFC)	Section 1, 2, 3	2021-01-18
3	E. Raclaru (SISW), C. Husar (SISW)	Section 4	2021-02-19
	E. Raclaru (SISW), C. Husar (SISW), J. Jaguemont (VUB)	Section 4.2	2021-02-19
4	F. Gao (UBFC), E. Raclaru (SISW), C. Husar (SISW)	Section 5	2021-02-19
5	F. Gao (UBFC), E. Raclaru (SISW), C. Husar (SISW)	Update and conclusions	2021-03-25
6	F. Gao (UBFC), E. Raclaru (SISW), C. Husar (SISW), W. Lhomme (ULille)	Finalization	2021-03-25

# Contents

1. Introduction.....	5
1.1 Fuel Cell Vehicle (FCV) description.....	5
1.2 Test methodology for model validation.....	6
1.3 Organisation method of the models for virtual testing .....	7
2. Modelling and EMR of the Mobypost .....	9
2.1 Structure of Mobypost Powertrain .....	9
2.2 Fuel cell system model.....	9
2.3 Battery model.....	11
2.4 DC-DC converter model .....	12
2.5 E-drive model .....	12
2.6 Mobypost vehicle model.....	14
2.7 Energy management strategy .....	15
3. Simulation and validation using Matlab-Simulink®.....	16
4. Simulation and validation using Simcenter Amesim®.....	21
4.1 Simulation and validation of the FCV model.....	21
4.2 Multi-level simulation of FCV .....	28
4.3 Cloud computing .....	32
4.4 Simcenter Amesim and Matlab Simulink simulation comparison .....	32
5. Discussion and Conclusions.....	36
5.1 Discussion.....	36
5.2 Conclusions .....	36
6. Deviations from Annex 1 .....	36
7. References.....	36
8. Acknowledgement.....	39
Appendix A – Quality Assurance .....	40
Appendix B – Abbreviations / Nomenclature.....	41

## Figures

Figure 1 FCV Mobypost powertrain structure [Ravey 2014].....	6
Figure 2 Driving cycle of the tested scenarios.....	7
Figure 3 FCV Mobypost modelling structure.....	9
Figure 4 Generic Fuel Cell Model .....	10
Figure 5 Fuel cell DEA1.0 polarisation curve from datasheet and simulation results.....	10
Figure 6 Battery model.....	11
Figure 7 Battery U24-12XP discharge curve from datasheet and simulation results. ....	11
Figure 8 The schematic diagram of boost converter.....	12
Figure 9 The EMR of boost converter.....	12
Figure 10 The EMR of e-drive.....	13
Figure 11 Mobypost energy management strategy.....	15
Figure 12 the EMR of Mobypost. ....	15
Figure 13 Matlab-Simulink® diagram of the Mobypost EMR model .....	16
Figure 14 Vehicle speed .....	17
Figure 15 Total power consumptions of two e-drives measured in the DC side .....	17
Figure 16 Batter SOC and H <sub>2</sub> tank SOC.....	19
Figure 17 Fuel cell output voltage, current, power.....	20
Figure 18 Battery output power.....	20
Figure 19 Simcenter Amesim implementation of Mobypost EMR model. ....	22
Figure 20 Vehicle speed. ....	23
Figure 21 E-drive motor rotating speed.....	23
Figure 22 Total power consumptions of two e-drives measured in the DC side. ....	24
Figure 23 DC Bus Energy transferred measured and simulated. ....	24

Figure 24 Battery SOC. ....	25
Figure 25 H2 tank SOC. ....	25
Figure 26 Fuel cell output voltage, current, power. ....	26
Figure 27 Battery output power. ....	27
Figure 28 Battery Energy used measured and simulated. ....	27
Figure 29 Representation of a 1st order Thévenin model. ....	28
Figure 30 EMR of the first battery model. ....	29
Figure 31 EMR of the dynamical electro-thermal model of a single cell. ....	29
Figure 32 DC bus side Energy provided for multi-level battery FCV. ....	30
Figure 33 Battery state-of-charge for two-level battery models. ....	30
Figure 34 Temperature evaluation for the level 2 battery model ....	30
Figure 35 Simcenter Amesim© implementation of Mobypost EMR model with multi-level battery model. ....	31
Figure 36 Simulation time-of-execution comparison between Cloud and local. ....	32
Figure 37 Computing machines performance specifications. ....	32
Figure 38 Vehicle speed. ....	33
Figure 39 E-drive motor rotating speed. ....	33
Figure 40 Total power consumptions of two e-drives measured in the DC side. ....	33
Figure 41 Battery SOC. ....	34
Figure 42 H2 tank SOC. ....	34
Figure 43 Fuel cell current. ....	34
Figure 44 Fuel cell voltage. ....	35
Figure 45 Battery power. ....	35

## Tables

Table 1 Technical specification of Mobypost used for tests .....	6
Table 2 EMR elements.....	8
Table 3 Technical specification of battery module U24-12XP used for Mobypost.....	9
Table 4 Technical specification of fuel cell system DEA1.0 used for Mobypost .....	9
Table 5: Project Partners.....	39
Table 6 List of Abbreviations / Nomenclature .....	41

# 1. Introduction

The objective of PANDA project is to provide a disruptive and open access model organization for an easy interconnection and change of models in the development process of electrified vehicles [PANDA 2019]. The model organisation is based on EMR (Energetic Macroscopic Representation) formalism [Bouscayrol 2012]. The formalism is implemented in the 1D simulation tools, Matlab-Simulink® and Simcenter Amesim®. The latter is an industrial simulation tool used in automotive industry. Models necessary for building a vehicle simulation were developed by PANDA partners. They developed multi-scale multi-domain models based on EMR formalism that can be introduced in a simulation architecture of electrified vehicles [PANDA D1.2].

This report is dedicated to a fuel cell vehicle (FCV) simulation and validation of vehicle simulation using EMR formalism by comparing simulation results with parameters measured on a real vehicle. The vehicle measured was Mobypost produced by UBFC and tested in FEMTO-ST research institute [Ravey 2014]. For this purpose, models were tuned using data provided by FEMTO-ST in order to be adapted to the tested vehicle.

Models were developed during previous stages of the project as follows:

- In Work Package 2 (WP2) – work package leader VUB, battery models were developed
- In Work Package 3 (WP3) – work package leader UTCN, electric drives models were developed
- In Work Package 4 (WP4) – work package leader SISW, car body model was developed

All models of the FCV were implemented and simulated in Matlab-Simulink® by UBFC. The FCV model has then be implemented in Simcenter Amesim® using the EMR library developed in PANDA [Husar 2019] [PANDA D4.1]. Test scenarios are adapted for the validation of individual models and validation of global vehicle performance. This report presents the system modeling developed using EMR formalism for systems from FCV and the global model of FCV developed using EMF formalism. System-level simulation of the FCV is performed based on the EMR formalism and the results of these simulations are compared with measured results and prove the efficiency and flexibility of the simulation platform developed in PANDA project. This fact gives confidence that the objective of PANDA project, to provide unified organisation of digital models for seamless integration in virtual testing for a FCV, is achieved.

## 1.1 Fuel Cell Vehicle (FCV) description

A fuel cell vehicle (FCV) is an electric vehicle that uses a fuel cell as primary source, in combination with a battery or supercapacitor as secondary source, to power its on-board electric motor [Eshani 218]. Fuel cells in vehicles generate electricity generally using oxygen from the air and compressed hydrogen. Most fuel cell vehicles are classified as zero-emissions vehicles that emit only water and heat, and are promising solutions in the electrified transportation applications. In automotive applications, proton exchange membrane fuel cell (PEMFC) appears to be the most suitable choice, because their working conditions at low temperature (50-80°C) allow the system to start up faster than those technologies using high-temperature FCs. Moreover, the solid state of their electrolyte (no leakage and low corrosion) and their high-power density make them fit for transport applications. According to the production of the hydrogen, they can also provide very good tank-to-wheel efficiency, compared with internal combustion engines.

The fuel cell stack is usually composed of several fuel cells in series to achieve relatedly high output voltage. Because FC stacking reduces the reliability and lifetime, a high voltage gain DC-DC converter is usually required to connect the FC stack to DC link. Moreover, a battery or supercapacitor is connected to the DC link to provide the instantaneous power required by the vehicle's acceleration and to absorb the regenerated energy from the wheel. The energy from the battery is transferred to one or several electrical motors which transforms the electrical energy to mechanical energy used for propulsion of the vehicle. Electrical motors are controlled by motor controllers to provide the necessary torque control for the vehicle.

The assembly electrical motor and motor controller is called electrical drive (e-drive) and for smaller power it is manufactured as single unit component.

“Mobypost” is a fuel cell vehicle developed by UBFC for the postal delivery application [Ravey 2014]. Mobypost vehicle is designed to ensure the last step in the delivery process, that is the delivery from local sorting centres to recipients. The hydrogen is locally produced by using the electric energy generated by photovoltaic technology to realize electrolysis of water.

The basic structure of Mobypost is shown in Figure 1. The Mobypost powertrain consists of a fuel cell stack followed by a DC-DC converter, a Li-ion battery pack directly connected to the DC link, two e-drives including two inverters driving two in-wheel permanent magnet synchronous motors (PMSM). There is no gearbox in Mobypost. Besides, a battery charger is equipped to charge the Li-ion battery when Mobypost is powered off. Figure 1 is the considered electrical architecture of the Mobypost, and is the system studied and validated in this report.

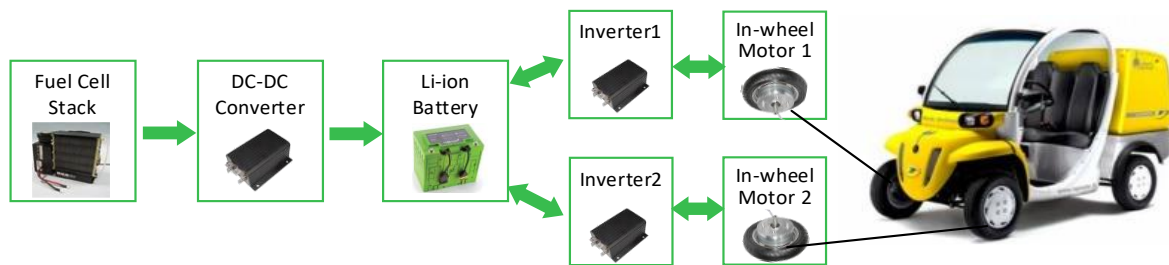


Figure 1 FCV Mobypost powertrain structure [Ravey 2014]

## 1.2 Test methodology for model validation

Testing methodologies used to perform the tests on the real vehicle, Mobypost were defined based on report [PANDA D1.6] and the specific needs from partners in charge with development of models. According to the specificity of each system, several scenarios were chosen to be measured which can cover the demands for all the partners. All modelled systems must be able to be used for simulation of their own performances and to be available to be used in global vehicle simulation for global performance of the vehicle. For this reason, the tests were done with the vehicle. In this report, a Mobypost vehicle was used for tests. General data for the vehicle and for the electric powertrain is given in Table 1.

Table 1 Technical specification of Mobypost used for tests

Number of seats	1	Electric motor technology	In-wheel PMSM
Weight (kg)	579	Electric motor nominal power (kW)	2
Fuel cell type	PEMFC	Electric motor peak torque (Nm) / maximum rpm	160 / 520
Fuel cell power (kW)	1.0	Battery Technology	Lithium-ion
Top speed (km/h)	60	Numbers of battery module	4
Wheelbase (mm)	270	Nominal module voltage (V)	12.8
Weight (kg)	579	Nominal capacity (Ah)	110

Models must reproduce the behaviour of the systems for normal use of a vehicle, there were chosen cycles of use from real postal delivery in France. The tests were carried out in FCLAB, Belfort, France. The tested driving cycles is shown in Figure 2.

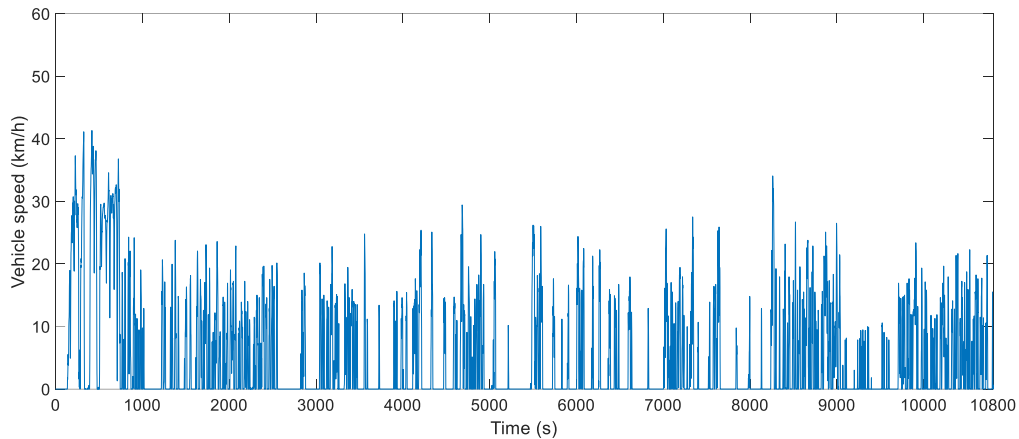


*Figure 2 Driving cycle of the tested scenarios*

### 1.3 Organisation method of the models for virtual testing

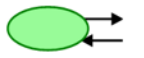
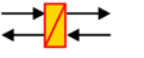




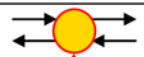


Organisation method for virtual and real testing define the methodology requirements for the development of multi-level model organization for PANDA objective. The method was described in report [PANDA D1.2]. The method imposes the following lines to be respected during the design and construction of the simulation platform:

- For models: Different models are defined for the same subsystem according to the objective of the study. In PANDA, a multi-level model approach is targeted to develop a N-level model organization. For the same subsystem, different models will thus be developed. Dynamical models (for transient states), static models (only for steady states) and quasi-static models are considered.
- For representation: In PANDA project functional description is imposed to avoid the need of co-simulation. Moreover, this choice enables to use pure causal description (i.e. physical causality, i.e. integral causality) [Hautier 2004] that leads to the reduction of the computation time [Moskwa 1997]. In this purpose, the EMR (Energetic Macroscopic Representation) formalism is selected [Bouscayrol 2012].
- For simulation: Most of the actual advanced simulation packages are defined in structural philosophy [PANDA D1.1]. In PANDA project the functional approach used is a challenging task, which requires some adaptation of actual simulation packages. Forward and backward approaches are used in function of the global objective, forward approach for dynamical models and backward approach for generally static or quasi-static models.

The EMR formalism is selected for the unified models' organisation because it is a graphical formalism (synthetic and unified view) based on a functional approach (flexibility) using exclusively the natural physical causality (adapted for real-time). Moreover, control schemes can be systematically deduced from the EMR of a subsystem and association rules have to also be defined to solve conflicts of association.

In order to organise the model of energy conversion system for control purpose, only 4 energetic functions are sufficient [Bouscayrol 2012]: source of energy, storage of energy, conversion of energy and distribution of energy. EMR is thus based on 4 basic pictograms to describe these functions (Table 2). Other pictograms have been defined to manipulate the models: switching between two models and power amplification to avoid model repetition, and 3 pictograms for controls (blue pictograms).

Table 2 EMR elements

	Source element (energy source)		Accumulation element (energy storage)		Indirect inversion (closed-loop control)
	Mono-domain conversion element		Mono-domain coupling element (energy distribution)		Direct inversion (open-loop control)
	Multi-domain conversion element		Multi-domain coupling element (energy distribution)		Coupling inversion (energy criteria)

The EMR of the complete system is thus composed of the connected EMR elements after solving the different conflicts of associations using the permutation and merging rules.

In PANDA project each partner developed his models of systems he is in charge with, using his own software solution Matlab-Simulink®. Models are developed using EMR formalism. After that, the models are transformed in Simcenter Amesim® with the help of SISW who developed a library with elements according to EMR rules for an easier implementation.



## 2. Modelling and EMR of the Mobypost

### 2.1 Structure of Mobypost Powertrain

The Mobypost developed by UBFC has a powertrain consisting of a Li-ion battery pack used as the main power source, a fuel cell stack used for charging the battery, a DC-DC converter used for boosting the fuel cell output voltage, two sets of e-drive composed of inverter and in-wheel PMSM, as shown in Figure 3 [Ravey 2014]. The battery pack is made up of four Li-ion battery modules in series, the U24-12XP produced by Valence, of which the parameters are given in Table 3. The fuel cell stack is the DEA 1.0 fuel cell system produced by MES S.A., of which the essential parameters are given in Table 4.

Therefore, the modelling of the Mobypost will focus on the fuel cell stack, DC-DC converter, Li-ion battery and the e-drive consisting of inverter and PMSM, and the vehicle's motion model, as shown in Figure 3. Besides, due to the multiple energy sources involved in FCV, the effective energy management strategy should be applied in the powertrain to coordinate the operation of fuel cell stack and battery pack.

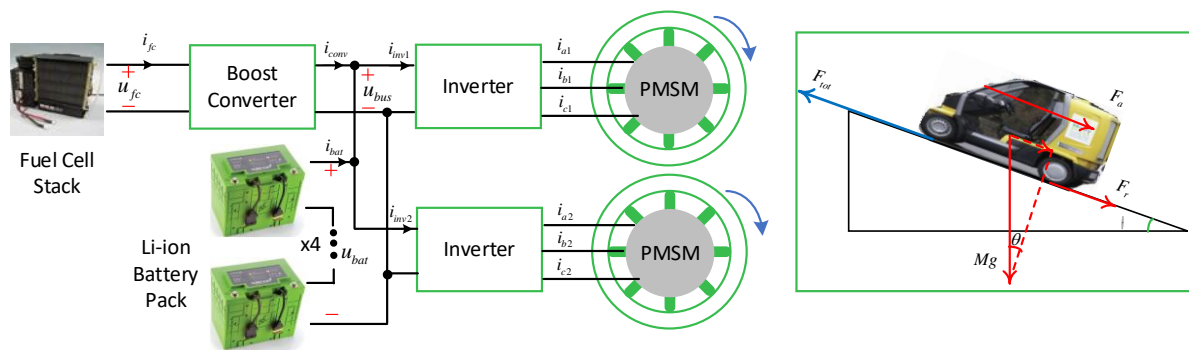


Figure 3 FCV Mobypost modelling structure

Table 3 Technical specification of battery module U24-12XP used for Mobypost

Nominal Module Voltage (V)	12.8	Energy Density (Wh/kg)	89
Nominal Capacity (Ah)	110	Max. Continuous Load Current (A)	150
Weight (kg)	15.8	Cut-off Voltage (V)	10
Dimension (mm)	260*172*225	DC internal resistance ( $\Omega$ )	0.006

Table 4 Technical specification of fuel cell system DEA1.0 used for Mobypost

Nominal Power [W]	1000	Number of cells	40
Stack Voltage Range [V]	24-38	Active Area [ $\text{cm}^2$ ]	61
Nominal Stack Voltage [V]	24	Total Weight (kg)	5.2
Nominal Stack Current [A]	45	Dimension (mm)	350*215*140
Hydrogen supply nominal pressure (bar relative)	0.5	Hydrogen supply minimum flow rate (Nlt/min)	13

### 2.2 Fuel cell system model

The fuel cell model used here is a generic fuel cell model that is well developed for the simulation purpose, of which the basic structure is given in Figure 4 [Tremblay 2009]. The fuel cell is represented by a controlled

voltage source in series with a resistor. The value of the voltage source  $E$  is computed by equation (1), and the fuel cell output voltage  $u_{fc}$  can be obtained from equation (2).

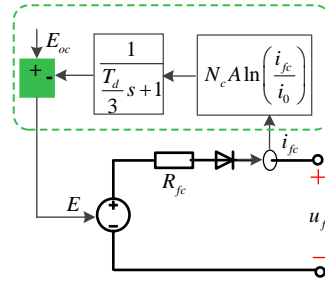


Figure 4 Generic Fuel Cell Model

$$E = E_{oc} - N_c \cdot A \cdot \ln\left(\frac{i_{fc}}{i_0}\right) \cdot \frac{1}{1/3 \cdot T_d s + 1} \quad (1)$$

$$u_{fc} = E - R_{fc} i_{fc} \quad (2)$$

$E_{oc}$  is the open circuit voltage,  $N_c$  is the number of cells,  $A$  is the Tafel slope,  $i_0$  is the exchange current,  $T_d$  is the response time,  $R_{fc}$  is the internal resistance,  $i_{fc}$  is the fuel cell current, and  $u_{fc}$  is the fuel cell output voltage [Tremblay 2009].

The parameters of equation (1) and equation (2) can be approximated based on the data extracted from the polarization curve in the fuel cell datasheet. Four parameters need to be identified, namely  $E_{oc}$ ,  $A$ ,  $R_{fc}$  and  $i_0$ , which requires four points taken from the fuel cell polarization curve. Two points are selected from activation region and the other two are from Ohmic region.

- Voltage at 0 A;
- Voltage at 1 A;
- Voltage at nominal current (35 A);
- Voltage at maximum current (60 A).

Figure 5 shows the polarization curves obtained from the developed fuel cell model and the datasheet [MES 2012]. It can be observed that the simulated voltage-current relationship of the fuel cell model is close to the experimental results, especially in the neighbourhood of the nominal operating point.

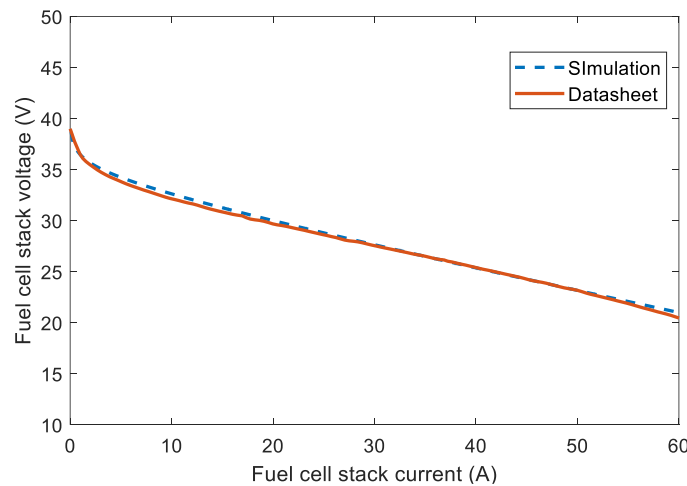


Figure 5 Fuel cell DEA1.0 polarisation curve from datasheet and simulation results.

## 2.3 Battery model

The battery model used in Task 4.4 is composed of a controlled voltage source in series with a constant resistance [Tremblay 2007]. The model structure is presented in Figure 6. The value of the voltage source depends on the battery SOC and can be represented by equation(3), where  $E$  is the open circuit voltage,  $E_0$  is the battery constant voltage,  $K$  is the polarization voltage,  $C_{bat}$  is the battery capacity ( $A \cdot h$ ),  $A$  is the exponential zone amplitude,  $B$  is the inverse of the exponential zone time constant, and  $R_{bat}$  is the internal resistance. The battery output voltage  $u_{bat}$  can thus be expressed by equation (4) depending on battery current  $i_{bat}$ . The SOC can be computed by equation (5).

$$E = E_0 - K \frac{C_{bat}}{C_{bat} - it} + Ae^{-B \cdot it} \quad (3)$$

$$u_{bat} = E - R_{bat}i_{bat} \quad (4)$$

$$SOC = \left(1 - \frac{\int i_{bat} dt}{3600C_{bat}}\right) \times 100\% \quad (5)$$

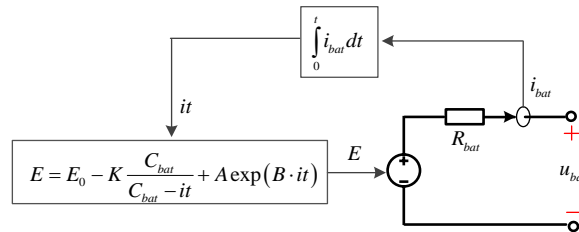


Figure 6 Battery model.

The parameters in equation (3) and (4) can be approximated based on the discharge and charge voltage profiles provided in battery datasheet. It needs to mention that the parameters in this model are derived from the discharge curve and the charge characteristics are assumed to be the same. The discharge voltage profile includes the exponential zone and the nominal zone. Three points are required to identify the parameters of equation (3) and (4), namely the fully charged voltage, the end of the exponential zone (voltage and charge) and the end of the nominal zone (voltage and charge). The internal resistance is chosen as the typical value provided by datasheet. Figure 7 shows the modelled discharge curve compared to the datasheet given curve at 0.5C discharge rate. It can be observed that two curves match well before 70% capacity. However, obvious deviations occur when the SOC is lower than 30%. This is one of the limitations in this model. Nevertheless, considering that Mobypost is not allowed to work under 30% SOC and this model can accurately represent the battery voltage profiles in Task 4.4. It is worth mentioning that the battery pack in Mobypost contains four battery modules in series, which means we must multiply the voltage by 4 to get the output voltage of battery pack.

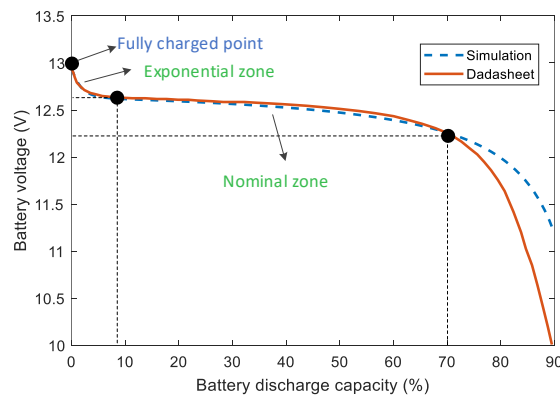


Figure 7 Battery U24-12XP discharge curve from datasheet and simulation results.

## 2.4 DC-DC converter model

A boost converter is used between the fuel cell stack and the DC link, as shown in Figure 8. A static model is applied to represent the behaviour of the boost converter, in which the switching dynamic is neglected and the switching effects are averaged over one switching cycle [Delarue 2003]. The mathematical model is described by using the following equations, where  $D$  is the duty cycle,  $u_{sw}$  is the voltage across the controlled switch, and the value of  $\eta_{conv}$  is the averaged efficiency of the power converter.

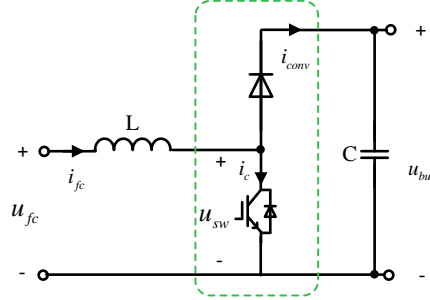


Figure 8 The schematic diagram of boost converter.

$$L \frac{di_{fc}}{dt} = u_{fc} - u_{sw} \rightarrow i_{fc} = \int \frac{1}{L} (u_{fc} - u_{sw}) dt \quad (6)$$

$$\begin{cases} u_{sw} = (1 - D)u_{bus} \\ i_{conv} = \eta_{conv}(1 - D)i_{fc} \end{cases} \quad (7)$$

The EMR representations of power converter model and its controller are represented in Figure 9.

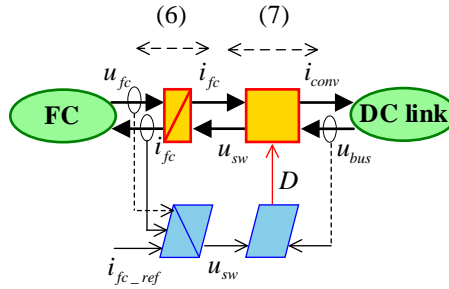


Figure 9 The EMR of boost converter.

## 2.5 E-drive model

The electric drive of Mobypost is constituted by a three-phase two-level inverter and an in-wheel PMSM. An averaged switch model is used to develop the inverter model. The modulation index is defined by the ratio of phase-to-phase voltages to the DC link voltage, as given in equation (8). Therefore, the output voltage of inverter can be computed by equation (9), where the matrix  $T_{l2p}$  converts the line voltages to phase voltages in three phase PMSM.

$$\mathbf{m}_{inv} = \begin{bmatrix} \frac{u_{ac}}{u_{bus}} & \frac{u_{bc}}{u_{bus}} \end{bmatrix}^T \quad (8)$$

$$\begin{bmatrix} u_a \\ u_b \\ u_c \end{bmatrix} = T_{l2p} \begin{bmatrix} u_{ac} \\ u_{bc} \end{bmatrix} = \frac{1}{3} \begin{bmatrix} 2 & -1 \\ -1 & 2 \\ -1 & -1 \end{bmatrix} u_{bus} \mathbf{m}_{inv} \quad (9)$$

A lumped parameter model in D-Q frame is used in which the saturation and the cross-saturation effects are not considered [PANDA D4.2]. The Concordia-Park transformation is used in this report for the power

conservation as shown in equation (10), where  $\omega_e$  is the electrical angular velocity,  $u_d, u_q$  are d, q axis voltages.

$$\begin{bmatrix} u_d \\ u_q \end{bmatrix} = \sqrt{\frac{2}{3}} \begin{bmatrix} \cos(\omega_e t) & \sin(\omega_e t) \\ -\sin(\omega_e t) & \cos(\omega_e t) \end{bmatrix} \begin{bmatrix} 1 & -\frac{1}{2} & -\frac{1}{2} \\ 0 & \frac{\sqrt{3}}{2} & -\frac{\sqrt{3}}{2} \end{bmatrix} \begin{bmatrix} u_a \\ u_b \\ u_c \end{bmatrix} \quad (10)$$

The PMSM voltage relationship is shown in equation (11) [Chen 2013].  $R_s$  is the resistance of the stator windings,  $\lambda_d, \lambda_q$  are the d, q axis flux linkages,  $i_d, i_q$  are d, q axis currents.

$$\begin{cases} u_d = R_s i_d + \dot{\lambda}_d - \omega_e \lambda_q \\ u_q = R_s i_q + \dot{\lambda}_q + \omega_e \lambda_d \end{cases} \quad (11)$$

$$\begin{cases} \lambda_d = L_d i_d + \lambda_f \\ \lambda_q = L_q i_q \end{cases} \quad (12)$$

$$\begin{bmatrix} \frac{di_d}{dt} \\ \frac{di_q}{dt} \end{bmatrix} = \begin{bmatrix} L_d^{-1} & 0 \\ 0 & L_q^{-1} \end{bmatrix} \left( \begin{bmatrix} u_d \\ u_q \end{bmatrix} - \begin{bmatrix} R_s & 0 \\ 0 & R_s \end{bmatrix} \begin{bmatrix} i_d \\ i_q \end{bmatrix} - \begin{bmatrix} e_d \\ e_q \end{bmatrix} \right) \quad (13)$$

$$\begin{cases} e_d = -\omega_e L_q i_q \\ e_q = \omega_e (L_d i_d + \lambda_f) \end{cases} \quad (14)$$

$$T_e = p(\lambda_f i_q + (L_d - L_q) i_q i_d) \quad (15)$$

The flux linkages are given by equation (12), where  $L_d, L_q$  are d, q axis inductances, and  $\lambda_f$  is the stator flux linkage induced by the permanent magnets of the rotor. Therefore, equation (13) and can be formulated based on equation (11) and equation (12). The back electromotive force of PMSM  $e_d, e_q$  can be computed by equation (14). The electromagnetic torque  $T_e$  can be computed by equation (15), where  $p$  is the number of pole pairs.

The e-drive model is presented in Figure 10 by using EMR formalism. The PMSM torque control is realized based on the maximum torque-per-amp (MTPA) control algorithm by following the equation (16) and equation (17) [Morimoto 1994], where  $i_m$  is the magnitude of armature current.

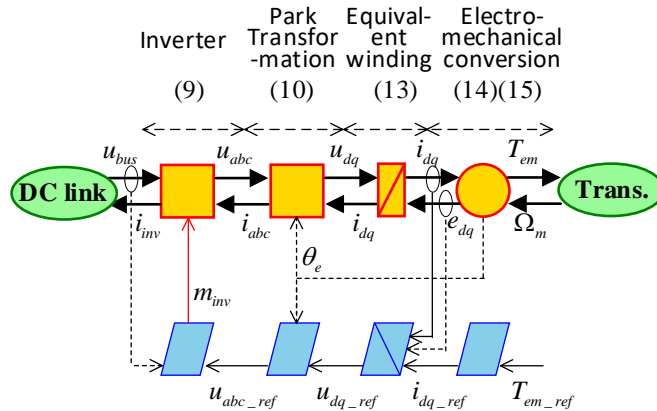


Figure 10 The EMR of e-drive.

$$i_d = \frac{\lambda_f}{4(L_q - L_d)} - \sqrt{\frac{\lambda_f^2}{16(L_q - L_d)^2} + \frac{i_m^2}{2}} \quad (16)$$

$$i_q = \sqrt{1.5i_m^2 - i_d^2} \quad (17)$$

## 2.6 Mobypost vehicle model

Due to the in-wheel PMSM used in Mobypost, the electromagnetic torque can be directly deployed to the wheel. The traction force and rotating of the speed of the wheel can be computed by equation (18), where  $r_{wh}$  is the radius of the wheel. In the model it is assumed that the wheels are not affected by slips and turns.

$$\begin{cases} \Omega_{wh} = \Omega_m = \frac{v_{veh}}{r_{wh}} \\ F_{wh} = \frac{T_{em}}{r_{wh}} \end{cases} \quad (18)$$

Two sets of e-drive are used in Mobypost, and the driving forces of two wheel ( $F_{wh1} + F_{wh2}$ ) are coupled with the braking force  $F_{br}$ . The total forces  $F_{tot}$  applied to the vehicle is computed by equation (19) and represented by a coupling element in EMR formalism.

$$F_{tot} = F_{wh1} + F_{wh2} + F_{br} \quad (19)$$

The vehicle velocity  $v_{veh}$  can be thus obtained by equation (20), in which  $F_{res}$  is the resistive force to the motion and  $M_{veh}$  is the vehicle mass. An accumulation element represents the accumulation of the energy in the chassis.

$$v_{veh} = \frac{1}{M_{veh}} \int (F_{tot} - F_{res}) dt \quad (20)$$

The road environment represents the resistive force  $F_{res}$ . This force is composed of the aerodynamic drag  $F_a$ , the rolling resistance  $F_r$  and the grading resistance  $F_g$ , as given in equation (21).  $F_a$  can be expressed as equation (22), where  $\rho$  is the air mass density,  $A_f$  is the equivalent front area of the Mobypost,  $C_d$  is the aerodynamic drag coefficient, and the  $v_{wind}$  is the wind speed.  $F_g$  and  $F_r$  can be obtained by using the equation (22), where the  $\theta$  is the slope and  $C_r$  is the rolling resistance coefficient.

$$F_{res} = F_a + F_r + F_g \quad (21)$$

$$\begin{cases} F_a = \frac{1}{2} \rho A_f C_d (v_{veh} + v_{wind})^2 \\ F_g = M_{veh} g \sin \theta \\ F_r = C_r M_{veh} g \cos \theta \end{cases} \quad (22)$$

From the EMR, an inversion-based control scheme can be obtained. Relation (20) is inverted by a closed-loop control shown in equation (23), where  $C(t)$  a controller to be defined and a PI controller is used in this report.

$$F_{tot\_ref} = C(t)(v_{veh\_ref} - v_{veh}) + F_{res} \quad (23)$$

Relation (19) is inverted using a distribution input  $k_{br}$  to distribute the forces between the brakes and the wheel, and using a distribution input  $k_{di}$  to distribute the driving forces between two wheels, as given in equation (24) and equation (25). In this report,  $k_{di}$  is chosen as 0.5 to distribute the forces equally to two wheels.  $k_{br}$  equals to 1 when  $F_{tot\_ref} < 0$  and the regenerative braking is not considered.

$$\begin{cases} F_{br\_ref} = k_{br} F_{tot\_ref} \\ F_{wh\_ref} = (1 - k_{br}) F_{tot\_ref} \end{cases} \quad (24)$$

$$\begin{cases} F_{wh1\_ref} = k_{di} F_{wh\_ref} \\ F_{wh2\_ref} = (1 - k_{di}) F_{wh\_ref} \end{cases} \quad (25)$$

Relation (18) is inverted by equation (26) to get the reference of the electromagnetic torque of each in-wheel PMSM.

$$\begin{cases} T_{em1\_ref} = r_{wh1} \cdot F_{wh1\_ref} \\ T_{em2\_ref} = r_{wh2} \cdot F_{wh2\_ref} \end{cases} \quad (26)$$

## 2.7 Energy management strategy

Mobypost has two energy sources in the powertrain, fuel cell and battery. Therefore, Mobypost needs an energy management system (EMS) to coordinate the operations of two sources. The EMS controls the start/stop of the fuel cell stack according to the battery SOC, and controls the output power of the fuel cell stack by deploying the closed-loop current control of the DC-DC converter. The rule-based energy management strategy is adopted in Mobypost, which can be described by a flow chart shown in Figure 11.

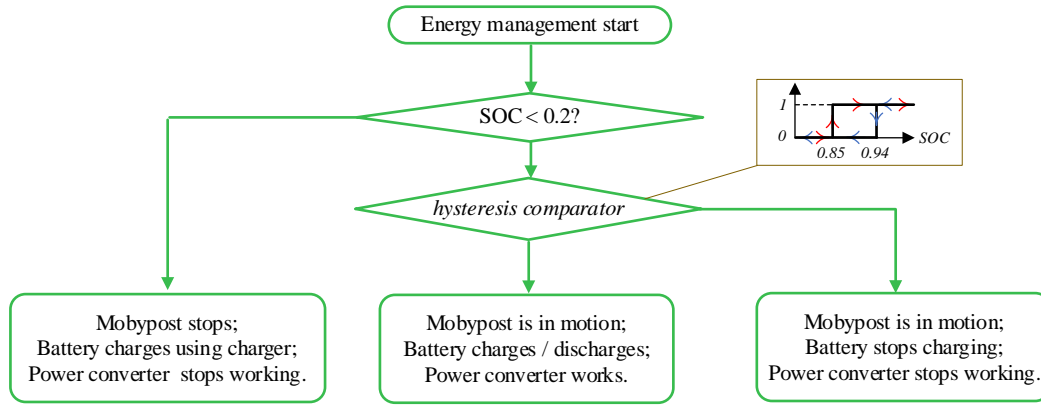


Figure 11 Mobypost energy management strategy.

By integrating the models developed in Section 2.2 to 2.7 using the EMR formalism, the EMR representation of Mobypost can be organized by Figure 12.

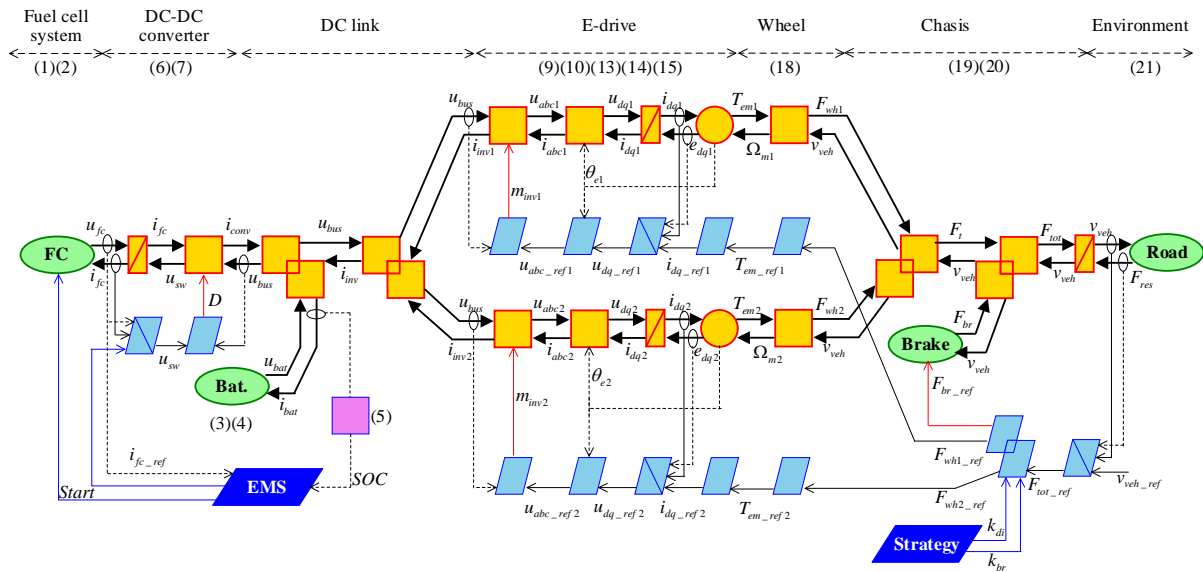


Figure 12 the EMR of Mobypost.

### 3. Simulation and validation using Matlab-Simulink®

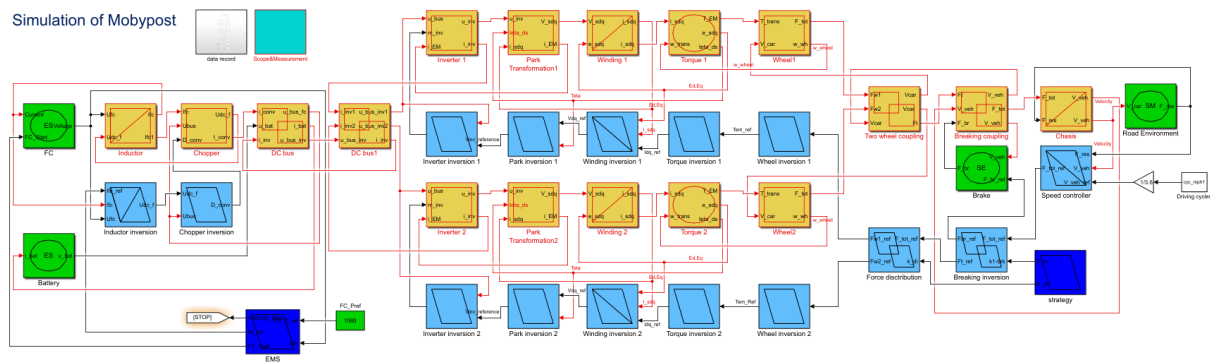
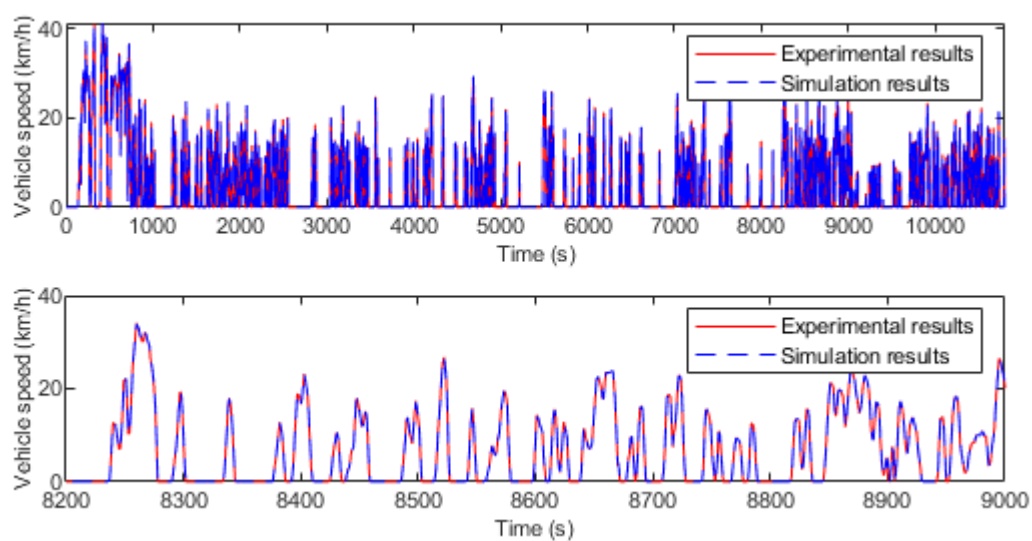


Figure 13 Matlab-Simulink® diagram of the Mobypost EMR model

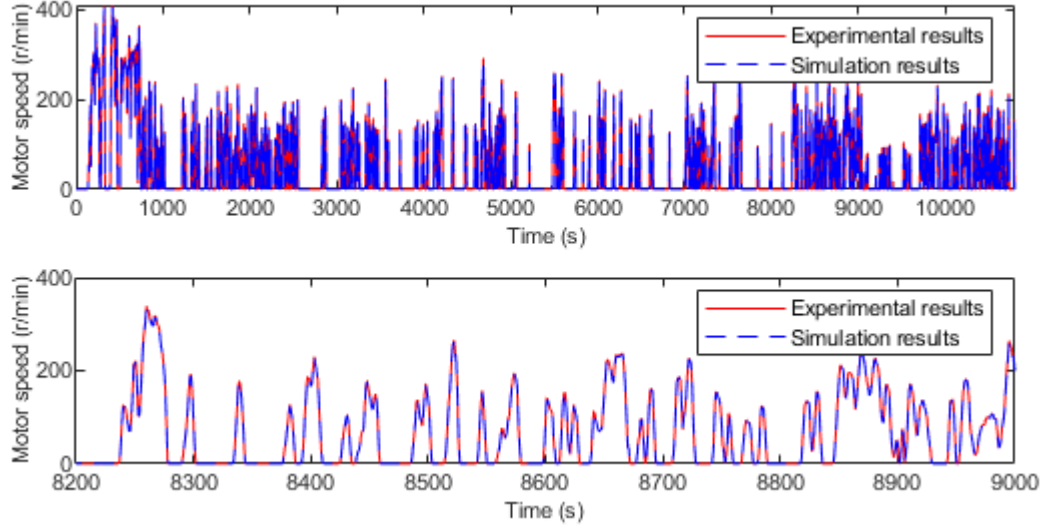
The driving cycle of test scenario is given in Figure 2, which is collected based on the daily postal delivery track from *La Poste*. The simulation is organized using the EMR formalism shown in Figure 12. The driving cycle is the input of the simulation, based on which the references of the electromagnetic torque of two e-drives are derived. The fuel cell and battery are operating under the control of the energy management system. The EMR of Mobypost is implemented in Simulink® environment, and simulated with a 1ms time-step for the driving cycle from 0 to 10800s. Figure 13 shows the Matlab-Simulink® block-diagram of the Mobypost EMR model.

Figure 14 to Figure 18 demonstrate the simulation results of the Mobypost EMR model together with the results of the Mobypost on road experiments. The dashed line is the simulation result, and the solid line is the experimental result. Figure 14(a) depicts the vehicle speed curves and Figure 14(b) depicts the rotating speed of the in-wheel PMSM of the right wheel, where the magnified curves are plotted at the bottom. The Mobypost model follows the reference speed rapidly and the errors are very small. Figure 14(a) illustrates the typical characteristics of the postal delivery driving cycles that contains many pauses and is thus the right time for the fuel cell to charge the battery to prolong the overall driving distance. Compared to the measured data, the simulation produces the consistent results.



(a) vehicle speed





(b) e-drive motor rotating speed

Figure 14 Vehicle speed

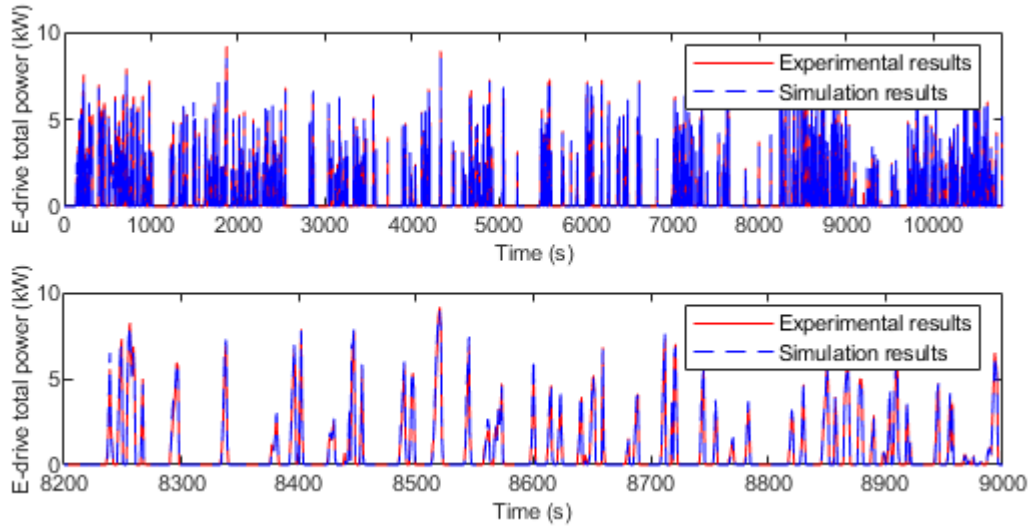


Figure 15 Total power consumptions of two e-drives measured in the DC side

The total power consumptions of two e-drives from the DC-link side are measured in both experimental test and simulation. The results are demonstrated in Figure 15. The top sub-figure is the power consumptions during the full tested driving cycles, the middle is the magnified waveforms between 8200s and 9000s in order to evaluate the performance of the developed model, and the bottom is the error between the measured ( $P_{dc-bus,meas}$ ) and simulated ( $P_{dc-bus,sim}$ ) power for every time step in percentages and is calculated according to the equation (27).

$$err(P_{dc-bus}) = \frac{|P_{dc-bus,meas} - P_{dc-bus,sim}|}{\max(P_{dc-bus,meas})} 100\% \quad (27)$$

The average error of the power is

$$mean(err(P_{dc-bus})) = 0.53 \% \quad (28)$$

From the view of EMR, the developed model can accurately represent the realistic power demands of the Mobypost.

The operating principles of the fuel cell and battery are presented in Figure 11, in which the energy management is implemented using the rule-based strategy based on the battery SOC. The variations of battery SOC and H2 tank SOC during the whole driving cycle are shown at the top of Figure 16 (a) and (b), while their errors are plotted at the bottom. The error between the measured ( $SOC_{bat,meas}$ ) and simulated ( $SOC_{bat,sim}$ ) battery state-of-charge is calculated according to equation (29).

$$err(SOC_{bat}) = \frac{|SOC_{bat,meas} - SOC_{bat,sim}|}{\max(SOC_{bat,meas})} 100\% \quad (29)$$

The average error of the SOC is

$$mean(err(SOC_{bat})) = 0.62 \%. \quad (30)$$

Similarly, the error between the measured ( $H_2SOC_{bat,meas}$ ) and simulated ( $H_2SOC_{bat,sim}$ ) fuel-cell tank state-of-charge is also indicated in (31) for every time step in percentages and is calculated according to equation (31).

$$err(H_2SOC_{bat}) = \frac{|H_2SOC_{bat,meas} - H_2SOC_{bat,sim}|}{\max(H_2SOC_{bat,meas})} 100\% \quad (31)$$

The average error of the SOC is

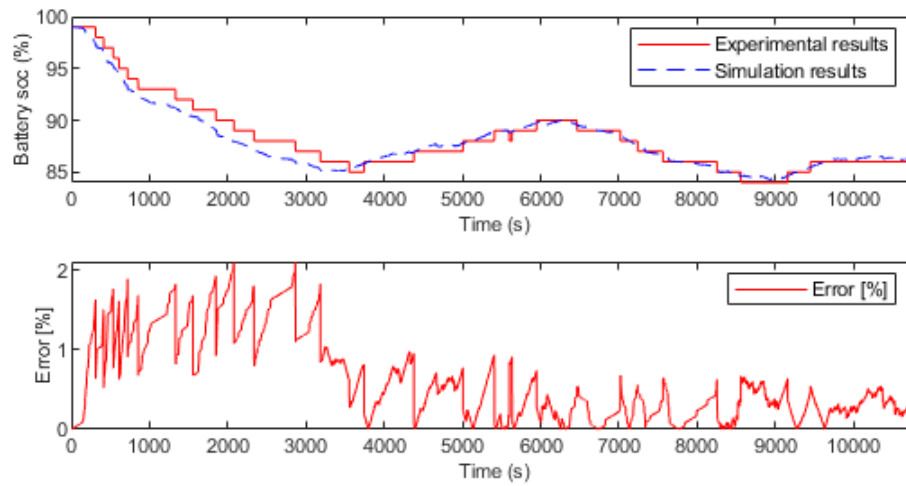
$$mean(err(H_2SOC_{bat})) = 0.48\%. \quad (32)$$

In Figure 16 (a), the simulated battery SOC shows accurate results and presents the consistent variations with the measured SOC. The differences can also be observed. On the one hand, the sampling rate of the measured SOC is too slow, and some information of the Mobypost SOC is missing; on the other hand, the simulation errors of the power demands will be accumulated in the computation of SOC. (b) H2 tank SOC

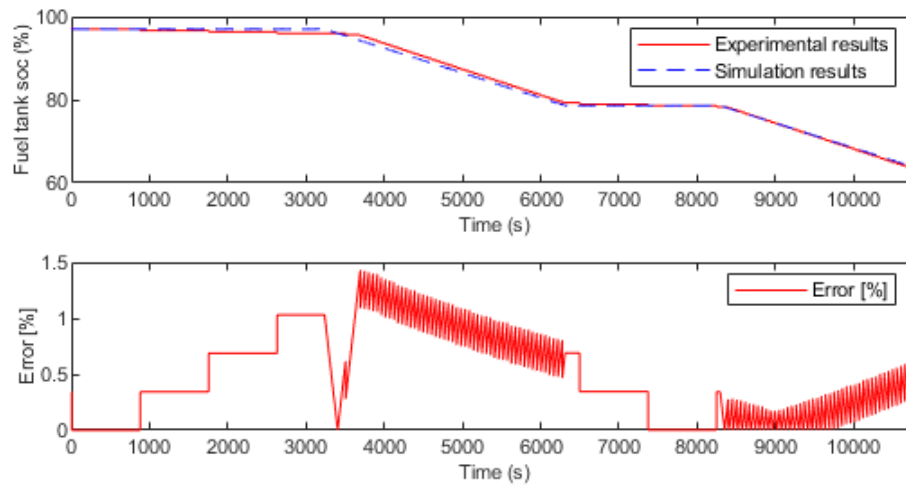
Figure 16 (b) depicts the results of the H2 tank SOC. The simulation also produces accurate results. Errors occurs in the period when the fuel cell stack is stopped. This is due to the power consumptions of auxiliary devices in fuel cell system, which is not considered in the simulation when fuel cell is not working. In general, the SOC of battery and H2 tank of the developed model are accurate in the system-level simulation of Mobypost.

Figure 17 shows the waveforms of fuel cell system output voltage, output current and the output power. The simulation results match the experimental results in the steady state. The differences occur at the starting and stopping stages of the fuel cell system. The start-up or shutdown of fuel cell is determined by the EMS based on the battery SOC. Therefore, the exact time of the start-up and shutdown can be inaccurate due to the simulation errors of the battery SOC. Moreover, the shutdown process of fuel cell involves complex electrochemistry mechanism which is not considered in the system-level fuel cell model developed here. Nevertheless, fuel cell model has satisfied accuracy regarding the system-level performance.

Figure 18 presents the variations of the battery output power in the tested driving cycles. The simulation results show consistency to the experimented results. Due to the errors of the SOC estimation, the deviations occur in start-up and shutdown process. The steady-state simulation results are accorded with the experiments. The developed model follows the real power consumptions of the vehicle's acceleration and deceleration. The slight differences can be observed in different driving conditions because the models of the power converters, e-drive and fuel cell system use the averaged efficiencies to represent the power losses in each component.

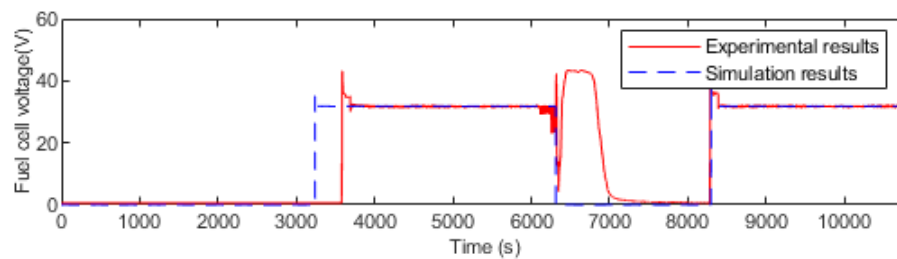


(a) Battery SOC

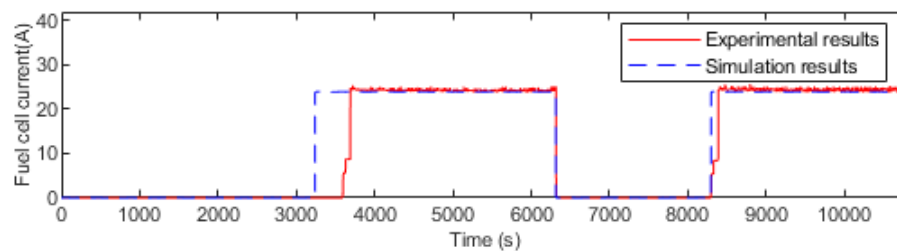


(b) H<sub>2</sub> tank SOC

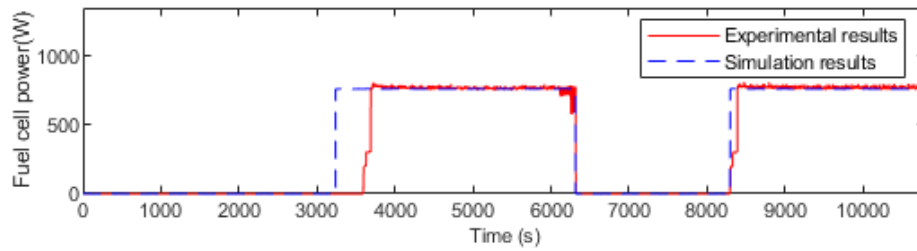
Figure 16 Batter SOC and H<sub>2</sub> tank SOC



(a) Fuel cell voltage



(b) Fuel cell current



(c) Fuel cell output power

Figure 17 Fuel cell output voltage, current, power.

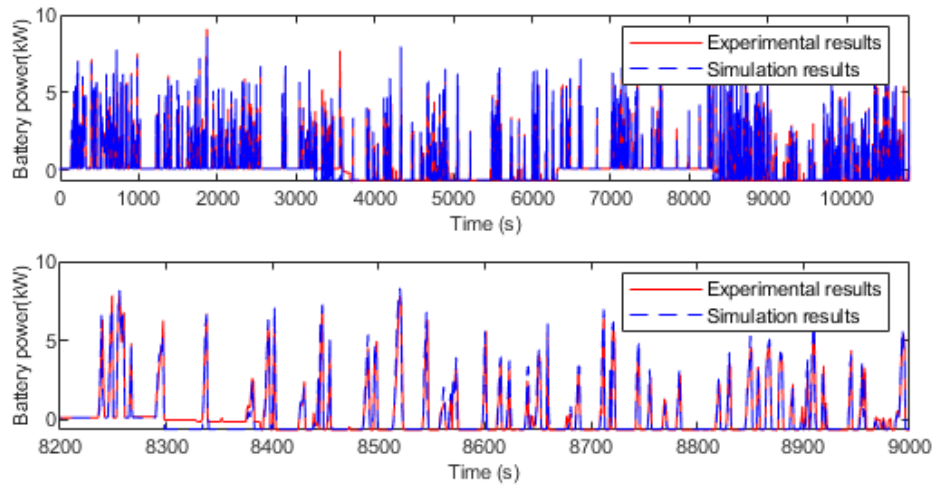


Figure 18 Battery output power.

Globally most of the errors between experimental results and simulation are lower than 2% that is within the acceptable deviation at the system level.

## 8. Acknowledgement

The author(s) would like to thank the partners in the project for their valuable comments on previous drafts and for performing the review.

*Table 5: Project Partners*

#	Type	Partner	Partner Full Name
1	UNIV	ULille	Université de Lille
2	IND	SISW	Siemens Industry Software SRL
3	UNIV	VUB	Vrije Universiteit Brussels
4	IND	VEEM	VALEO Equipement Electriques Moteur SAS
5	UNIV	UTCN	Universitatea Tehnica Cluj Napoca
6	SME	TY	Tajfun HIL (Typhoon HIL)
8	UNIV	UBFC	Université Bourgogne Franche-Comté
9	SME	UNR	Uniresearch BV
10	IND	RTR	Renault Technologie Roumanie
11	SME	Bluways	BlueWays International bva
12	IND	TUV	TUV SUD Battery Testing GmbH



This project has received funding from the European Union's Horizon2020 research and innovation programme under Grant Agreement no. 824256.

## Appendix A – Quality Assurance

As part of the quality assurance procedure:

- The following questions should be answered by all reviewers (WP Leader, peer reviewer 1, peer reviewer 2 and the technical coordinator);
- Questions answered with NO should be motivated. The author will then make an updated version of the Deliverable. When all reviewers have answered all questions with YES, only then the Deliverable can be submitted to the EC.

**NOTE: For public documents this Quality Assurance part will be removed before publication.**

Question	WP Leader	Peer reviewer 1	Peer reviewer 2	Technical Coordinator
	Cristi Irimia	Walter Lhomme	Gabriel-Mihai Sirbu	Alain Bouscayrol
1. Do you accept this deliverable as it is?	YES	YES	YES	YES
2. Is the deliverable completely ready? If not, please indicate and motivate required changes.	YES	YES	YES	YES
3. Does this deliverable correspond to the DoW?	YES	YES	YES	YES
4. Is the Deliverable in line with the PANDA objectives?	YES	YES	YES	YES
a. WP Objectives?	YES	YES	YES	YES
b. Task Objectives?	YES	YES	YES	YES
5. Is the technical quality sufficient?	YES	YES	YES	YES

## Appendix B – Abbreviations / Nomenclature

*Table 6 List of Abbreviations / Nomenclature*

Symbol / Shortname	
FCV	Fuel cell vehicle
PEMFC	Proton exchange membrane fuel cell
EMR	Energetic Macroscopic Representation
PMSM	Permanent Magnet Synchronous Motor
SOC	State of Charge
EMS	Energy management system